

Robust excitation of ^{229}Th via generalized composite pulses: Compensating generic errors across arbitrary pulse shapes

Rui Zhao(赵睿), and Yingdan Wang(王颖丹)

Citation: Chin. Phys. B, 2026, 35 (**6**): 063201. DOI: 10.1088/1674-1056/ae4e8d
http://cpb.iphy.ac.cn; http://iopscience.iop.org/cpb

What follows is a list of articles you may be interested in

Measuring the Coulomb time shift in high-order harmonic generation

Shengjun Yue(岳生俊), Siqi Song(宋思琦), Ruofeng Zhong(钟若峰), Jiangkun Li(李江坤), Haiyuan Yu(于海元), and Hongchuan Du(杜洪川)
Chin. Phys. B, 2026, 35 (**4**): 043201. DOI: 10.1088/1674-1056/ae1951

Nondestructive detection of atom counts in laser-trapped ^{171}Yb atoms

Congcong Tian(田聪聪), Qiang Zhu(朱强), Bing Wang(王兵), Dezhi Xiong(熊德智), Zhuanxian Xiong(熊转贤), Lingxiang He(贺凌翔), and Baolong Lyu(吕宝龙)
Chin. Phys. B, 2025, 34 (**2**): 023201. DOI: 10.1088/1674-1056/ad9e9d

A miniaturized spin-exchange relaxation-free atomic magnetometer based on uniform light field

Jiajie Li(李佳洁), Xiujie Fang(房秀杰), Renjie Li(李任杰), Baodong Chen(陈宝栋), Yueyang Zhai(翟跃阳), and Ying Liu(刘颖)
Chin. Phys. B, 2023, 32 (**5**): 053201. DOI: 10.1088/1674-1056/aca7f2

Integrated, reliable laser system for an ^{87}Rb cold atom fountain clock

Zhen Zhang(张镇), Jing-Feng Xiang(项静峰), Bin Xu(徐斌), Pan Feng(冯盼), Guang-Wei Sun(孙广伟),Yi-Ming Meng(孟一鸣), Si-Min-Da Deng(邓思敏达), Wei Ren(任伟),Jin-Yin Wan(万金银), and De-Sheng Lü(吕德胜)
Chin. Phys. B, 2023, 32 (**1**): 013202. DOI: 10.1088/1674-1056/ac9e95

Transient electromagnetically induced transparency spectroscopy of ^{87}Rb atoms in buffer gas

Zi-Shan Xu(徐子珊), Han-Mu Wang(王汉睦), Zeng-Li Ba(巴曾立), and Hong-Ping Liu(刘红平)
Chin. Phys. B, 2022, 31 (**7**): 073201. DOI: 10.1088/1674-1056/ac4748

SPECIAL TOPIC — Advance in thorium nuclear optical clocks

Robust excitation of ^{229}Th via generalized composite pulses: Compensating generic errors across arbitrary pulse shapes

Rui Zhao(赵睿)[1,2] and Yingdan Wang(王颖丹)[1,†]

[1] *Institute of Theoretical Physics, Chinese Academy of Sciences, Beijing* 100190, *China*
[2] *School of Physical Sciences, University of Chinese Academy of Sciences, Beijing* 100049, *China*

(Received 19 January 2026; revised manuscript received 28 February 2026; accepted manuscript online 7 March 2026)

High-fidelity coherent control is a universal challenge due to complex errors and imperfect pulse shapes. Here, we propose a generalized composite pulses scheme independent of pulse profile to correct generic errors. This approach could simultaneously compensate for pulse area errors, detuning, and phase imperfections. We demonstrate its application in the direct laser excitation of the ^{229}Th nucleus isomer state, and show a significant improvement in the robustness against various operation errors, such as detuning, phase error, and pulse area error.

Keywords: thorium-229, isomeric state, nuclear excitation, composite pulses

PACS: 32.80.Qk, 06.30.Ft, 03.67.Bg

DOI: 10.1088/1674-1056/ae4e8d **CSTR:** 32038.14.CPB.ae4e8d

1. Introduction

The ^{229}Th nuclear optical clock represents a central frontier in precision metrology.[1,2] Recently, continuous-wave (CW) vacuum-ultraviolet (VUV) lasers capable of driving this transition have been realized.[3] These pioneering experiments have brought the system into the regime of coherent control, as the achievable nuclear Rabi frequency ($\Omega \approx \pi \times 91$ Hz) is now capable of exceeding the effective laser linewidth ($\sim$100 Hz).[3] However, high-fidelity excitation is currently impeded by a critical disparity: the achievable Rabi frequency remains significantly smaller than the uncertainty of the transition frequency (~ 2 kHz).[2] This uncertainty leads to a potentially large effective detuning, preventing a standard π-pulse from achieving high-efficiency excitation. Furthermore, the temporal profiles of VUV pulses, particularly in the recent pulsed laser excitation experiments,[2,4,5] are inherently difficult to shape perfectly, introducing pulse area errors that further degrade the excitation fidelity.

To mitigate the deleterious effects of large detuning and pulse shape imperfections, composite pulse (CP) techniques naturally emerge as a promising solution.[6,7] Originally developed in nuclear magnetic resonance (NMR),[8] these methods have been widely adopted across quantum information science, including trapped-ion quantum computing,[9,10] neutral-atom interferometry,[11,12] superconducting circuits,[13] and solid-state spin qubits.[14,15] In principle, broadband CP sequences could also compensate for the unknown detuning encountered in ^{229}Th experiments. However, implementing CP sequences in the vacuum ultraviolet (VUV) regime ($\sim$ 150 nm) introduces additional complexity. Despite recent advances,[16,17] precise phase modulation in the VUV remains technically demanding, standing in sharp contrast to the mature control available in the microwave or visible domains. Furthermore, the modulation process itself can introduce unavoidable phase inaccuracies. Therefore, a robust strategy for exciting ^{229}Th is required to correct both detuning and pulse shape distortions while simultaneously tolerating phase errors intrinsic to VUV generation and manipulation.

The standard composite pulse approach employs sequences of pulses with tailored phases to cancel error terms in the system's evolution. This typically requires deriving the explicit form of the time-evolution operator to identify conditions to cancel the low-order error derivatives. However, unlike resonant pulses, the evolution under a detuned pulse generally lacks an analytical solution except for special cases such as square or hyperbolic pulse shapes. To address the complex scenario of Thorium isomer excitation, we develop in this work a generalized CP method that is independent of the pulse profile. Instead of using an explicit evolution operator, we adopt a general parameterized form of an SU(2) operator as suggested in Ref. [18]. Our approach distinguishes itself by its universality; it compensates generalized error parameters across arbitrary and potentially distorted pulse shapes. While previous work by the Vitanov group has demonstrated error correction for arbitrary waveforms through evolution-parameter optimization[18] and later extended robustness to phase errors,[19] their solutions remain implicitly dependent on the pulse profile when treating detuning. In contrast, our

†Corresponding author. E-mail: yingdan.wang@itp.ac.cn

© 2026 Chinese Physical Society and IOP Publishing Ltd. All rights, including for text and data mining, AI training, and similar technologies, are reserved.

method directly targets the physical error parameter z by imposing vanishing conditions on the derivatives of the excitation probability, thereby ensuring strict independence from the pulse shape. As a result, we show that high-fidelity nuclear excitation of ^{229}Th can be achieved despite significant detuning, pulse-shape distortions, and technical phase modulation errors, offering a robust pathway toward future nuclear clock experiments.

The outline of our paper is as follows. Section 2 discusses the physical model of ^{229}Th excitation and the limitations of conventional CP pulses. Section 3 presents the derivation of the generalized CP technique for arbitrary pulse shapes and details the simultaneous compensation of multiple error types. Section 4 discusses experimental feasibility and broader applications, and Section 5 provides the conclusion.

2. Physical model and conventional composite pulses

To design robust control sequences, we first establish the theoretical model for the direct laser excitation of the nuclear system. The energy of the second excited state of the ^{229}Th nucleus (29 keV) is significantly higher than that of the first excited state (8.4 eV).[2] Furthermore, the first excited state has an intrinsic radiative lifetime of approximately 10^3 s,[1,2] which is significantly longer than the excitation interaction time (10^{-2} s to seconds scale). Consequently, the process of direct laser excitation of $^{229\mathrm{m}}$Th can be effectively modeled as the interaction between an external field and a two-level system,[20] governed by the Schrödinger equation

$$\mathrm{i}\hbar\frac{\partial}{\partial t}|\psi(t)\rangle = \hat{H}(t)|\psi(t)\rangle. \tag{1}$$

Here, the total Hamiltonian $\hat{H}(t) = \hat{H}_{\mathrm{N}} + \hat{H}_{\mathrm{I}}(t)$ comprises the nuclear Hamiltonian (incorporating effects from external static electric or magnetic fields) and the interaction Hamiltonian describing the coupling between the nucleus and the applied laser field. Assuming the laser intensity is sufficiently low that the diagonal terms of the interaction Hamiltonian can be neglected (*i.e.*, considering only single-photon excitation processes) and applying the rotating wave approximation, the Hamiltonian is given by

$$\hat{H}(t) = \frac{\hbar}{2}\begin{pmatrix} \Delta(t) & \Omega(t) \\ \Omega(t) & -\Delta(t) \end{pmatrix}, \tag{2}$$

where $\Delta(t) = \omega(t) - \omega_0$ is the detuning between the laser angular frequency $\omega(t)$ and the transition angular frequency ω_0, and $\Omega(t)$ is the corresponding Rabi frequency.

Since the Hamiltonian is traceless ($\mathrm{Tr}[\hat{H}(t)] = 0$) and Hermitian, it acts as a generator of the $\mathfrak{su}(2)$ algebra. Consequently, the propagator $\hat{U}(t) = \mathcal{T}\exp\left(-\frac{\mathrm{i}}{\hbar}\int_0^t \hat{H}(t')\,\mathrm{d}t'\right)$ belongs to the special unitary group SU(2), which can be parameterized as[18]

$$\hat{U}(t) = \begin{pmatrix} a(t) & b(t) \\ -b^*(t) & a^*(t) \end{pmatrix}, \tag{3}$$

where $a(t)$ and $b(t)$ are Cayley–Klein parameters satisfying $|a(t)|^2 + |b(t)|^2 = 1$. In the following sections, all propagators are considered at the final time t_{f}, and for simplicity, the explicit time dependence t_{f} will be omitted. Assuming the system starts in the ground state, the corresponding excitation probability is $P = |U_{21}|^2 = 1 - |U_{11}|^2$.

At resonance ($\Delta = 0$), where $\left[\hat{H}(t_1), \hat{H}(t_2)\right] = 0$, the propagator simplifies to

$$\hat{U} = \begin{pmatrix} \cos\frac{A}{2} & -\mathrm{i}\sin\frac{A}{2} \\ -\mathrm{i}\sin\frac{A}{2} & \cos\frac{A}{2} \end{pmatrix}, \tag{4}$$

where the pulse area is defined as $A = \int_0^{t_{\mathrm{f}}} \Omega(t')\,\mathrm{d}t'$. The excitation probability is then given by

$$P = \sin^2\frac{A}{2}. \tag{5}$$

In the ideal case, a pulse area of $A = \pi$ drives the system to full excitation ($P = 1$), corresponding to the standard π-pulse technique. Consider a pulse area error α, such that $A \to A(1+\alpha)$. For a single π pulse, the excitation probability takes the form

$$P(\alpha) = \sin^2\left(\frac{\pi(1+\alpha)}{2}\right) = 1 - \frac{\pi^2}{4}\alpha^2 + \mathcal{O}(\alpha^4). \tag{6}$$

The presence of the quadratic term ($-\frac{\pi^2}{4}\alpha^2$) implies that the excitation fidelity of a single π-pulse is degraded to second order by the pulse area error.

In contrast, composite pulse sequences use the relative phases as an optimization parameter to mitigate the effects of experimental errors arising from laser bandwidth fluctuations, intensity instabilities, and other experimental factors.[6,21] Laser phase modulation techniques allow for the generation of an arbitrary phase ϕ in the Rabi frequency, such that $\Omega(t) \to \Omega(t)\,\mathrm{e}^{\mathrm{i}\phi}$. The corresponding propagator becomes[7]

$$\hat{U} = \begin{pmatrix} a & b\,\mathrm{e}^{\mathrm{i}\phi} \\ -b^*\,\mathrm{e}^{-\mathrm{i}\phi} & a^* \end{pmatrix}. \tag{7}$$

For a sequence of N pulses that differ only in their phases, the total propagator is

$$U^{(N)} = U(\phi_{\mathrm{N}})U(\phi_{N-1})\cdots U(\phi_2)U(\phi_1), \tag{8}$$

where ϕ_n denotes the phase of the nth pulse. Since only the relative phases affect the excitation dynamics, we set $\phi_1 = 0$.

Assuming the composite sequence consists of constituent pulses each with a nominal area $A = \pi$, an odd number of pulses, $N = 2n+1$ (where $n = 1, 2, \ldots$), is required to fully excite the system. For simplicity, we impose a symmetric phase distribution: $\phi_k = \phi_{N+1-k}$ ($k = 1, 2, \ldots, n$), and analyze the excitation probability represented by $U_{11}^{(N)}$ (*i.e.*, $P = 1 - |U_{11}^{(N)}|^2$).[21]

To achieve an excitation probability curve with maximum robustness against error z, we expand $U_{11}^{(N)}$ as a multivariate series around $z=0$ and set the j-th order coefficient to zero:

$$\left.\frac{\partial^j U_{11}^{(N)}}{\partial z^j}\right|_{z=0} = 0. \tag{9}$$

Consequently, the sensitivity of the excitation probability to the error z is suppressed up to the $2j$-th order.

2.1. Compensation of pulse area errors

For laser excitation of ^{229}Th, the required wavelength lies within the VUV range around 150 nm. Lasers in this band face challenges in achieving both high intensity and long duration simultaneously, potentially leading to pulse area errors.[2,4,5]

The assumptions $N=2n+1$ and $\phi_k=\phi_{N+1-k}$ $(k=1,2,\ldots,n)$ ensure that all even-order derivatives vanish with respect to the pulse area error.[21] To maximize robustness, we set the first N odd-order coefficients of $U_{11}^{(N)}$ to zero

$$\left.\frac{\partial^j U_{11}^{(N)}}{\partial \alpha^j}\right|_{\alpha=0} = 0, \quad j=1,3,\ldots,N. \tag{10}$$

For a sequence with $N=3$, $U_{11}^{(3)}$ is given by

$$\begin{aligned} U_{11}^{(3)} &= [\cos(\phi_2)+\cos(\pi\alpha)(1+\cos(\phi_2))]\sin\left(\frac{\pi\alpha}{2}\right) \\ &= \frac{\pi}{2}[1+2\cos(\phi_2)]\,\alpha \\ &\quad -\frac{\pi^3}{48}[13+14\cos(\phi_2)]\,\alpha^3+\mathcal{O}(\alpha^4). \end{aligned} \tag{11}$$

Setting the first-order coefficient of $U_{11}^{(3)}$ to zero yields the optimal solutions $\phi_2=\pm 2\pi/3$. The pulse sequence corresponding to $\phi_2=2\pi/3$ is schematically illustrated in Fig. 1.

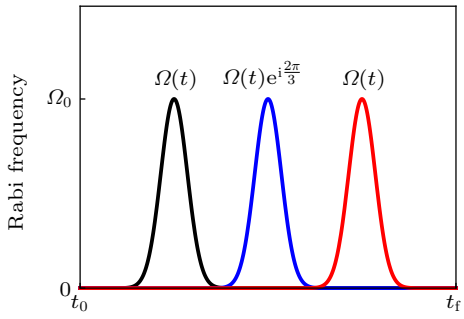


Fig. 1. Schematic diagram of the $N=3$ composite pulse sequence. The phases for the three component pulses are set to $\phi_1=\phi_3=0$ and $\phi_2=2\pi/3$, respectively. This phase configuration corresponds to the optimal solution for cancelling the first-order error term derived in the text.

With this phase configuration, the propagator element expands as

$$U_{11}^{(3)} = -\frac{\pi^3}{8}\alpha^3+\mathcal{O}(\alpha^4). \tag{12}$$

The corresponding excitation probability reduces to

$$P^{(3)} = 1-\frac{\pi^6}{64}\alpha^6+\mathcal{O}(\alpha^8). \tag{13}$$

This result indicates that the excitation probability is insensitive to pulse-area errors up to the fourth order (strictly speaking, the error scales as α^6, implying robustness up to the fifth order). As clearly visible in Fig. 2, the $N=3$ curve exhibits a distinct 'flat-top' feature, standing in sharp contrast to the narrow peak of the single-pulse ($N=1$) benchmark.

An analytical expression for the phases of any sequence with an odd number of pulses is given by[21]

$$\phi_k^{(N)} = \left(N+1-2\left\lfloor\frac{k+1}{2}\right\rfloor\right)\left\lfloor\frac{k}{2}\right\rfloor\frac{\pi}{N}, \tag{14}$$

where $k=1,2,\ldots,N$. This solution provides a simple expression for the excitation probability:

$$P^{(N)} = 1-\cos^{2N}\left(\frac{\pi(1+\alpha)}{2}\right). \tag{15}$$

Expanding the probability in a series around $\alpha=0$, we have

$$P^{(N)} = 1-\frac{\pi^{2N}}{4^N}\alpha^{2N}+\mathcal{O}(\alpha^{2N+2}).$$

Figure 2 illustrates the excitation probability as a function of the relative pulse area error α for various sequence lengths. We observe that the excitation profiles exhibit a distinct 'flat-top' feature around $\alpha=0$. As the number of pulses N increases from 1 to 13, this high-fidelity plateau broadens significantly, maintaining near-unity excitation probability even for large error magnitudes (*e.g.*, $\alpha>0.6$ for $N=13$). This visual broadening directly confirms the higher-order error cancellation derived in Eq. (14).

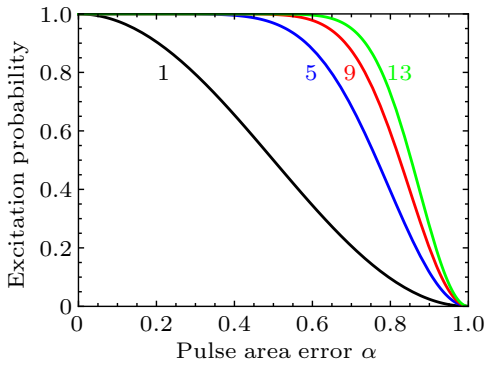


Fig. 2. Sequences with $N=1$, 3 , 5, 9, 13. Excitation probability *versus* relative pulse area error α. Increased N widens the high-fidelity region ($P\approx 1$).

2.2. Compensation of detuning

While pulse area errors are a significant concern, nuclear energy levels are highly stable compared to electronic levels but can still be shifted by external electromagnetic fields. The precise nuclear energy levels of Th ions experience slight shifts depending on their ionization state due to variations in the electron–nucleus interaction.[22,23] On the other hand, temperature fluctuations, defects, surface effects, and complex nucleus–electron–environment interactions in the host crystal

can perturb these energy levels, introducing unavoidable frequency shifts in solid-state nuclear clocks.[24,25] Additionally, laser linewidth contributes to spectral uncertainty. These factors introduce another critical source of error: detuning between the laser frequency and the nuclear transition frequency.

Even in the presence of only static detuning Δ, few cases yield analytical solutions. For square pulses with Rabi frequency $\Omega(t) = \Omega_0$, the propagator elements are

$$\begin{aligned} a &= \cos\left(\frac{A}{2}\sqrt{1+\beta^2}\right) - \frac{\mathrm{i}\beta}{\sqrt{1+\beta^2}}\sin\left(\frac{A}{2}\sqrt{1+\beta^2}\right), \\ b &= -\frac{\mathrm{i}}{\sqrt{1+\beta^2}}\sin\left(\frac{A}{2}\sqrt{1+\beta^2}\right), \end{aligned} \tag{16}$$

where the pulse area is $A = \Omega_0 T$ and $\beta = \Delta/\Omega_0$ is the normalized detuning.

For hyperbolic-secant pulses with Rabi frequency $\Omega(t) = \Omega_0 \mathrm{sech}(t/T)$, the Rosen–Zener solution exists[26] for $t_\mathrm{f} \to \infty$,

$$\begin{aligned} a &= \frac{\Gamma(\frac{1}{2} - \mathrm{i}\frac{A\beta}{2\pi})^2}{\Gamma(\frac{1}{2} - \mathrm{i}\frac{A\beta}{2\pi} - \frac{A}{2\pi})\Gamma(\frac{1}{2} - \mathrm{i}\frac{A\beta}{2\pi} + \frac{A}{2\pi})}, \\ b &= -\mathrm{i}\frac{\sin\frac{A}{2\pi}}{\cosh\frac{A\beta}{2\pi}}, \end{aligned} \tag{17}$$

where the pulse area is $A = \pi\Omega_0 T$.

Simple analytical solutions for phase are generally unavailable for detuning compensation. Consequently, we numerically solve the trigonometric equations

$$\left.\frac{\partial^j U_{11}^{(N)}}{\partial \Delta^j}\right|_{\Delta=0} = 0, \quad j = 1, 2, \ldots, n. \tag{18}$$

We identify multiple solutions that satisfy conditions for both square pulses and hyperbolic-secant pulses. The determined phases are listed in Table 1. For compactness, we set the reference phase $\phi_1 = 0$ and present only the unique non-zero phases $(\phi_2, \ldots, \phi_{n+1})$ in vector notation, from which the full symmetric sequence can be reconstructed. Figure 3 depicts the excitation probability loss $1 - P$ as a function of detuning Δ for both (a) square and (b) hyperbolic-secant pulses. We observed that while the single-pulse benchmark ($N = 1$) degrades rapidly with detuning, the composite sequences carve out a broad 'high-fidelity basin' where the loss is suppressed below 10^{-4}. As the pulse number N increases, this low-loss window significantly widens, demonstrating that the robustness against detuning is systematically enhanced regardless of the specific pulse profile.

For excitation of ^{229}Th, the CW laser can reach an achievable Rabi frequency of $\Omega \approx \pi \times 91$ Hz. As illustrated in Fig. 3, composite pulse sequences with $N = 5$ can maintain more than 95% excitation probability even with a detuning of 140 Hz, which is already larger than the laser bandwidth of 100 Hz. These results suggest that it is possible to construct phase sequences capable of compensating for generic errors in arbitrary pulse shapes, which leads us to the generalized scheme presented in the next section.

Table 1. Optimized phases for detuning compensation (symmetric sequences).

N	Unique phases $(\phi_2, \ldots, \phi_{n+1})^\dagger$
3	$(\pi/3)$
5	$(-\pi/6, \pi/3)$
7	$(-0.5527, \pi/3, 0.5527)$
9	$(0.0789, 2.6621, 2.1037, -2.2015)$
11	$(-1.4421, -3.0531, 0.0130, 1.6931, 2.2372)$
13	$(0.1296, 3.1336, 2.2806, -1.1738, 1.8468, 0.8305)$

† We set $\phi_1 = 0$ and $\phi_k = \phi_{N+1-k}$.

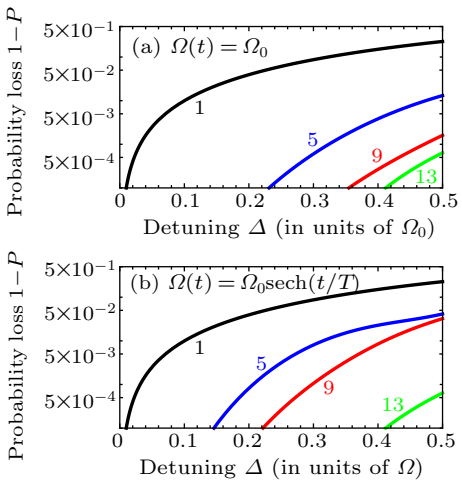


Fig. 3. Sequences with $N = 1, 5, 9, 13$. Excitation probability loss $1 - P$ *versus* detuning Δ: (a) square pulses and (b) hyperbolic-secant pulses. Increased N widens the low-loss region.

3. Generalized composite pulses for arbitrary pulse shapes

In experiments, multiple error sources, such as pulse area error and detuning, often coexist, contributing collectively to a reduction in excitation probability across various pulse shapes. Only a few pulse shapes, such as rectangular and hyperbolic-secant pulses, possess analytical solutions for detuning compensation. Moreover, perfect pulse shapes are experimentally unattainable. Other pulse shapes lack analytical solutions. Therefore, we aim to develop composite pulse sequences capable of addressing diverse error sources across arbitrary pulse shapes.

Building upon the waveform-independent parameterization introduced by Genov *et al.*,[18] we extend this formalism to explicitly target a generic error parameter z. The propagator for a constituent pulse with phase ϕ is parameterized as

$$U(z) = \begin{pmatrix} q(z)\,\mathrm{e}^{\mathrm{i}x(z)} & p(z)\,\mathrm{e}^{\mathrm{i}y(z)}\,\mathrm{e}^{\mathrm{i}\phi} \\ -p(z)\,\mathrm{e}^{-\mathrm{i}y(z)}\,\mathrm{e}^{-\mathrm{i}\phi} & q(z)\,\mathrm{e}^{-\mathrm{i}x(z)} \end{pmatrix}, \tag{19}$$

where $p(z)$, $q(z)$, $x(z)$, and $y(z)$ are real functions satisfying the normalization condition $p(z)^2 + q(z)^2 = 1$. For a perfect π

pulse (*i.e.*, $z=0$), the propagator reduces to

$$U(0)=\begin{pmatrix}0 & -\mathrm{i}\\ -\mathrm{i} & 0\end{pmatrix}, \tag{20}$$

yielding the boundary conditions: $p(0)=1$, $q(0)=0$, $x(0)=0$, $y(0)=-\pi/2$.

For brevity, we omit the explicit argument z hereafter. The recurrence relations for the matrix elements are given by

$$\begin{aligned} U_{11}^{(N)} &= q\mathrm{e}^{\mathrm{i}x}U_{11}^{(N-1)}-p\mathrm{e}^{\mathrm{i}y}\mathrm{e}^{\mathrm{i}\phi_N}U_{12}^{(N-1)*},\\ U_{12}^{(N)} &= q\mathrm{e}^{\mathrm{i}x}U_{12}^{(N-1)}+p\mathrm{e}^{\mathrm{i}y}\mathrm{e}^{\mathrm{i}\phi_N}U_{11}^{(N-1)*}. \end{aligned} \tag{21}$$

Using mathematical induction, $U_{11}^{(N)}$ is independent of y and can be expressed as (see Appendix A for proof):

$$U_{11}^{(N)}=\sum_{j=0}^{\lfloor N/2\rfloor}c_{nj}(\{\phi\},x)\,q^{2j+N-2\lfloor N/2\rfloor}, \tag{22}$$

where $\{\phi\}$ denotes the set of phases and $\lfloor\cdot\rfloor$ denotes the floor function.

3.1. Compensation method for generalized error parameters

To explicitly determine the phases that ensure robustness, we apply the derivative cancellation condition to the generalized propagator. By invoking the multivariate chain rule, the j-th order total derivative of $U_{11}^{(N)}$ with respect to the error parameter z can be expanded as

$$\frac{\partial^j U_{11}^{(N)}}{\partial z^j}=\sum_{0\le k_1+k_2\le j}C_{k_1,k_2}\frac{\partial^{(k_1+k_2)}U_{11}^{(N)}}{\partial q^{k_1}\partial x^{k_2}}\mathcal{D}_{k_1,k_2}(z), \tag{23}$$

where C_{k_1,k_2} are combinatorial coefficients and $\mathcal{D}_{k_1,k_2}(z)$ denotes terms containing the derivatives of the mapping functions $q(z)$ and $x(z)$. Crucially, the partial derivatives $\partial^{(k_1+k_2)}U_{11}^{(N)}/\partial q^{k_1}\partial x^{k_2}$ depend solely on the sequence structure and are independent of the physical parameters, including pulse shape and error type. Consequently, nullifying these partial derivatives ensures robust performance regardless of the specific physical model encoded in $\mathcal{D}_{k_1,k_2}(z)$. Using the boundary conditions, the even j_1-th derivative of $U_{11}^{(N)}$ vanishes at $z=0$. We can derive equations for arbitrary errors and pulse shapes by setting the following trigonometric equations to zero:

$$\left.\frac{\partial^{(j_1+j_2)}U_{11}^{(N)}}{\partial q^{j_1}\partial x^{j_2}}\right|_{q=0,x=0}=0, \tag{24}$$

for odd integers j_1 ($j_1=1,3,\ldots$) and all integers $j_2\ge 0$. This suppresses the sensitivity of the excitation probability to error z up to the order of j_1+j_2.

Take $N=5$ as an example; the first two derivatives are

$$U_{11}^{(5)\prime}=(1+2\cos(\phi_2-\phi_3)+2\cos(2\phi_2-\phi_3))\,q', \tag{25}$$

$$\begin{aligned} U_{11}^{(5)\prime\prime}=&(1+2\cos(\phi_2-\phi_3)+2\cos(2\phi_2-\phi_3))\,q''\\ &+2\mathrm{i}\,(1-2\cos(\phi_2-\phi_3)+2\cos(2\phi_2-\phi_3))\,x'q'. \end{aligned} \tag{26}$$

The corresponding trigonometric equations are

$$\begin{aligned} &1+2\cos(\phi_2-\phi_3)+2\cos(2\phi_2-\phi_3)=0,\\ &1-2\cos(\phi_2-\phi_3)+2\cos(2\phi_2-\phi_3)=0. \end{aligned} \tag{27}$$

When $\phi_2=-\pi/6$ and $\phi_3=\pi/3$, the first two-order terms of $U_{11}^{(5)}$ with respect to z are eliminated, and the excitation rate's sensitivity to z becomes 6th order.

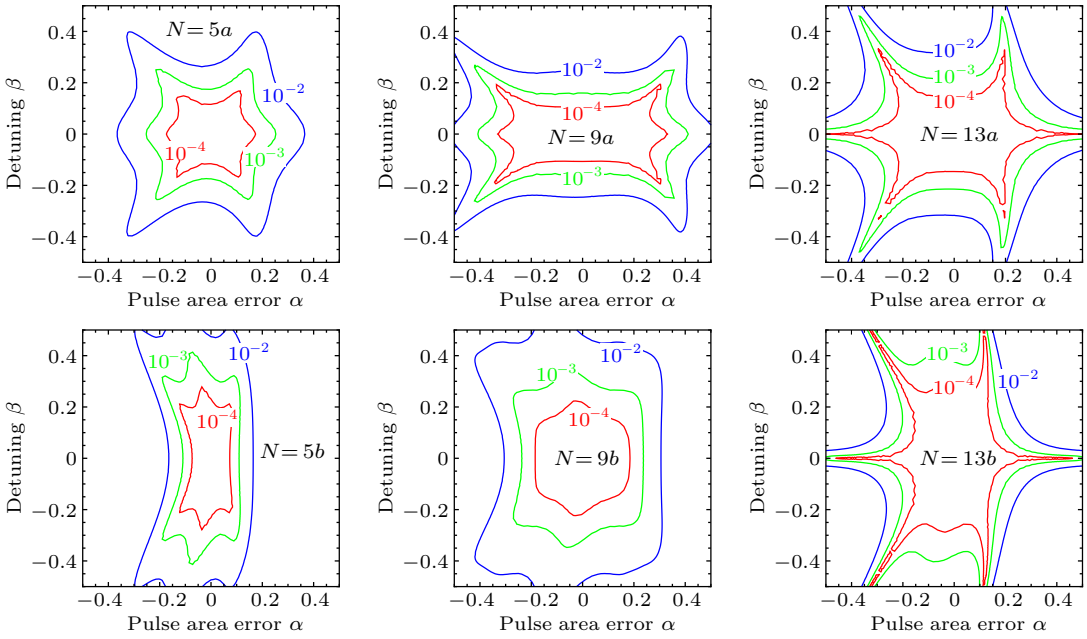


Fig. 4. Contour plots of excitation probability loss $1-P$ *versus* pulse area error α and detuning Δ, for sequences simultaneously compensating generic errors. From left to right: 5, 9, and 13 pulses. Contour lines represent $1-P=10^{-2}$ (blue), 10^{-3} (green), and 10^{-4} (red), '*a*' and '*b*' denote sequences optimized for better performance regarding pulse area error or detuning, respectively.

Table 2. Optimized phases for generic error compensation.

Sequence	Unique phases $(\phi_2,\ldots,\phi_{n+1})^{\dagger}$
5*a*	$(5\pi/6,\pi/3)$
5*b*	$(-\pi/6,\pi/3)$
7*a*	$(-1.4572,\pi/3,1.4572)$
7*b*	$(0.1399,-2.8619,-1.6748)$
9*a*	$(-1.4884,1.9138,-2.2171,-1.2713)$
9*b*	$(0.4195,-1.7893,0.5840,1.3043)$
13*a*	$(2.7470,1.3620,2.7878,0.9391,-2.7625,-1.3011)$
13*b*	$(2.6736,1.6309,2.9928,0.7278,0.5467,-1.3709)$

$^{\dagger}\phi_1 = 0$; Note: '*a*' and '*b*' denote sequences with prioritized robustness against pulse area error and detuning, respectively.

The optimized phase sequences are listed in Table 2. Following the convention established in Section 2, we present only the unique non-zero phases. For $N = 5$, 7, 9, the sensitivity of the probability is suppressed to the 6th, 8th, and 10th order, respectively. We take pulse area error α and detuning Δ as examples of errors. In Table 2, indices '*a*' and '*b*' denote sequences optimized for better performance regarding pulse area error or detuning, respectively. For $N = 13$, sensitivity is suppressed to the 12th order. Figure 4 illustrates the excitation fidelity contours in the (α, Δ) plane. We observe that as the sequence length N increases, the region enclosed by the red contour (indicating an error threshold of 10^{-4}) expands significantly. By $N = 13$, this ultra-high-fidelity region covers a substantial range of parameter space, demonstrating that the composite pulses can achieve precision comparable to ideal conditions even under moderate experimental imperfections.

For CW lasers, composite pulse sequences with $N = 9$ can maintain an excitation probability of more than 99%, even with a detuning of 140 Hz and a pulse area error of 30%, which is already larger than the laser bandwidth of 100 Hz and substantially larger than the pulse area error caused by deviations from perfect square pulses. This demonstrates the effectiveness of composite pulses in the robust excitation of ^{229}Th.

3.2. Compensation of phase errors

However, the validity of the composite pulse sequences discussed in the previous sections relies on the assumption of precise phase modulation. In practice, phase error, denoted by γ, must be constrained to within 0.1%–1% for short sequences, with even more stringent requirements for longer sequences. The phase modulation of VUV lasers is still a developing technology, making such precise control challenging[16,17] (the specific hardware limitations are discussed in detail in Section 4). This can result in small but non-negligible phase errors in practical implementations.

To address this limitation and enhance experimental feasibility, we model the phase error as a multiplicative perturbation: $\phi \to \phi(1+\gamma)$. $U_{11}^{(N)}$ remains independent of y and can be expressed as

$$U_{11}^{(N)} = \sum_{j=0}^{\lfloor N/2 \rfloor} c_{nj}\left(\{\phi(1+\gamma)\},x\right) q^{2j+N-2\lfloor N/2 \rfloor}. \tag{28}$$

To achieve robustness against phase imperfections, we require the excitation probability to be insensitive to γ to leading order. This is achieved by setting the mixed partial derivative with respect to the generalized error parameter q and the phase error γ to zero:

$$\frac{\partial^2 U_{11}^{(N)}}{\partial q \partial \gamma} = 0. \tag{29}$$

By solving Eq. (29) in conjunction with the conditions for generic error compensation Eq. (23), we derive composite sequences that are simultaneously robust against arbitrary pulse shape errors (such as pulse area and detuning) and phase modulation errors.

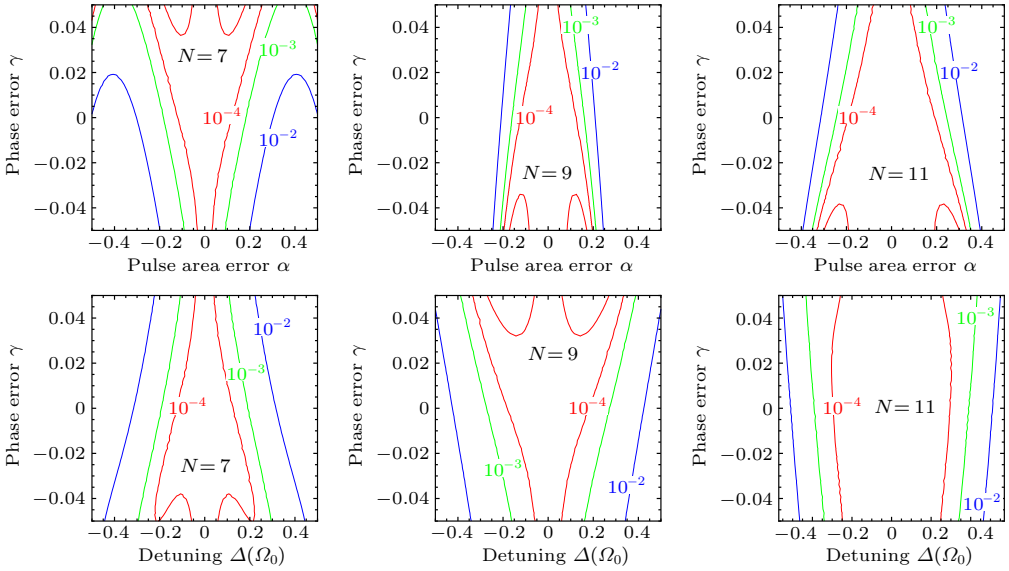


Fig. 5. Contour plots of excitation probability loss $(1-P)$ *versus* pulse area error α, detuning Δ, and phase error γ for sequences simultaneously compensating for generic errors. From left to right: results for $N = 7$, 9, and 11 pulses. Contour lines represent loss levels of 10^{-2} (blue), 10^{-3} (green), and 10^{-4} (red).

Numerical results for selected sequences are summarized in Table 3, using the same compact notation. For sequence lengths $N = 7, 9, 11$, the sensitivity of the excitation probability is suppressed up to the 6th, 8th, and 10th orders, respectively. Figure 5 displays the robustness map in the presence of phase errors (γ). Even with the inclusion of this additional error source, the blue (10^{-2}) and green (10^{-3}) contours retain a wide coverage area, showing minimal shrinkage compared to the ideal phase case. This persistence of the high-fidelity zones (bounded by the red lines) confirms that the proposed sequences effectively decouple the excitation efficiency from phase modulation imperfections. Notably, the tolerance for phase error extends beyond 2%, significantly relaxing the constraints on the experimental control system. This confirms that our generalized approach can effectively handle the full complexity of experimental error sources.

Table 3. Phases for simultaneous error compensation.

N	Unique phases $(\phi_2, \ldots, \phi_{n+1})^{\dagger}$
7	$(-1.4572, \pi/3, 1.4572)$
9	$(0.8433, -0.8558, 0.3214, 0.1887)$
11	$(1.8690, -0.7389, -1.0119, 0.9794, -0.4582)$

† See Table 1 for definitions.

4. Experimental feasibility and broader applications

Regarding the experimental realization of these composite pulse sequences for ^{229}Th, specific technical challenges must be addressed. The primary difficulty lies in achieving fast and precise phase modulation in the VUV regime. Currently, direct phase modulation at such short VUV wavelengths using conventional electro-optic or acousto-optic modulators is hindered by severe material absorption and low optical damage thresholds. A feasible experimental approach is to apply the phase shifts to the fundamental visible or infrared driving lasers before they undergo nonlinear frequency up-conversion processes, such as high-harmonic generation (HHG) or four-wave mixing.[16,17] However, a major difficulty in this approach is that the highly nonlinear up-conversion process can amplify the fundamental phase noise and introduce complex, waveform-dependent phase distortions. These technical challenges motivate our generalized scheme: its independence from pulse profiles and high tolerance to phase errors (γ) make it naturally suited for VUV composite pulse generation.

Beyond the direct laser excitation of the ^{229}Th nucleus, our generalized scheme constitutes a universal methodology applicable to broader quantum control scenarios. In fact, similar universal composite pulses have already proven highly successful in correcting arbitrary field errors in rare-earth-ion-doped crystals.[18] Following this paradigm, our specific waveform-independent sequences can be directly applied to other well-established platforms. For instance, in superconducting circuits[13] and neutral-atom arrays,[12,27] microwave and optical pulses often suffer from unknown distortions and spatial variations. Testing our scheme in these accessible systems could provide immediate experimental verification of its robustness before high-fidelity VUV phase-modulation technology fully matures.

5. Conclusion

In this work, we propose a generalized composite pulses scheme designed to correct generic errors across arbitrary pulse profiles. By utilizing a waveform-independent parameterization and enforcing derivative cancellation, our method serves as a versatile control tool capable of enhancing fidelity under complex experimental imperfections. We analyze the utility of this technique using the direct laser excitation of the ^{229}Th nucleus as a stringent test case, where hardware limitations are particularly severe.

Our results demonstrate that this generalized methodology provides a powerful tool to mitigate the specific challenges posed by current vacuum-ultraviolet laser technology. By robustly compensating for pulse area inaccuracies, large effective detunings, and phase modulation errors exceeding 2%, our approach significantly relaxes the stringent requirements on experimental stability and control precision. Consequently, this work offers a practical pathway to enhance the feasibility of observing the nuclear transition and supports future progress toward ^{229}Th nuclear optical clocks. Beyond this specific application, the inherent universality of our method makes it a valuable asset for diverse quantum control platforms where pulse shaping capabilities are limited.

Appendix A: Recursive relations and parameter independence of the propagator

A crucial feature of our optimization strategy is that the matrix element $U_{11}^{(N)}$ is mathematically independent of the parameter y. In this appendix, we provide a rigorous proof of this property based on the recursive relations derived from the SU(2) formalism. This independence simplifies the control problem, justifying the formulation of the error compensation conditions in Section 3 solely in terms of q and x.

We define the single-pulse propagator for the k-th pulse as

$$U_k = \begin{pmatrix} q\mathrm{e}^{\mathrm{i}x} & p\mathrm{e}^{\mathrm{i}(y+\phi_k)} \\ -p\mathrm{e}^{-\mathrm{i}(y+\phi_k)} & q\mathrm{e}^{-\mathrm{i}x} \end{pmatrix}. \tag{A1}$$

The total propagator follows the recurrence $U^{(k)} = U_k U^{(k-1)}$. Using the relations $U_{22} = U_{11}^*$ and $U_{21} = -U_{12}^*$, we derive the recurrence relations

$$U_{11}^{(k)} = q\mathrm{e}^{\mathrm{i}x} U_{11}^{(k-1)} - p\mathrm{e}^{\mathrm{i}(y+\phi_k)} [U_{12}^{(k-1)}]^*, \tag{A2}$$

$$U_{12}^{(k)} = q\mathrm{e}^{\mathrm{i}x}U_{12}^{(k-1)} + p\mathrm{e}^{\mathrm{i}(y+\phi_k)}[U_{11}^{(k-1)}]^*. \tag{A3}$$

We prove by induction that $U_{11}^{(N)}$ depends only on $q, x, \{\phi\}$, while $U_{12}^{(N)}$ takes the form $\mathrm{e}^{\mathrm{i}y} \times \tilde{U}_{12}$, where $\tilde{U}_{12}$ is independent of y.

Base case ($N = 1$)**:** For the first pulse ($\phi_1 = 0$)

$$U_{11}^{(1)} = q\mathrm{e}^{\mathrm{i}x}, \quad U_{12}^{(1)} = p\mathrm{e}^{\mathrm{i}y}. \tag{A4}$$

Obviously, $U_{11}^{(1)}$ depends only on q, x, and $U_{12}^{(1)}$ contains the factor $\mathrm{e}^{\mathrm{i}y}$.

Inductive step: Assume the property holds for $k-1$: $U_{11}^{(k-1)}$ is independent of y, and $U_{12}^{(k-1)} = \mathrm{e}^{\mathrm{i}y}\tilde{U}_{12}^{(k-1)}$. Substituting these into Eq. (A2):

$$\begin{aligned} U_{11}^{(k)} &= q\mathrm{e}^{\mathrm{i}x}U_{11}^{(k-1)} - p\mathrm{e}^{\mathrm{i}(y+\phi_k)}[\mathrm{e}^{\mathrm{i}y}\tilde{U}_{12}^{(k-1)}]^* \\ &= q\mathrm{e}^{\mathrm{i}x}U_{11}^{(k-1)} - p\mathrm{e}^{\mathrm{i}\phi_k}\mathrm{e}^{\mathrm{i}y}\mathrm{e}^{-\mathrm{i}y}[\tilde{U}_{12}^{(k-1)}]^* \\ &= q\mathrm{e}^{\mathrm{i}x}U_{11}^{(k-1)} - p\mathrm{e}^{\mathrm{i}\phi_k}[\tilde{U}_{12}^{(k-1)}]^*. \end{aligned} \tag{A5}$$

The term $\mathrm{e}^{\mathrm{i}y}\mathrm{e}^{-\mathrm{i}y} = 1$ cancels out perfectly. Thus, $U_{11}^{(k)}$ remains independent of y.

Similarly, substituting into Eq. (A3):

$$\begin{aligned} U_{12}^{(k)} &= q\mathrm{e}^{\mathrm{i}x}[\mathrm{e}^{\mathrm{i}y}\tilde{U}_{12}^{(k-1)}] + p\mathrm{e}^{\mathrm{i}(y+\phi_k)}[U_{11}^{(k-1)}]^* \\ &= \mathrm{e}^{\mathrm{i}y}\left\{q\mathrm{e}^{\mathrm{i}x}\tilde{U}_{12}^{(k-1)} + p\mathrm{e}^{\mathrm{i}\phi_k}[U_{11}^{(k-1)}]^*\right\}. \end{aligned} \tag{A6}$$

This confirms that $U_{12}^{(k)}$ retains the global phase factor $\mathrm{e}^{\mathrm{i}y}$.

Conclusion: We have demonstrated that the matrix element $U_{11}^{(N)}$ is strictly independent of the parameter y. Consequently, the derivatives $\partial^j U_{11}^{(N)}/\partial z^j$ derived in the main text depend only on the variations of q and x. This allows us to construct universal composite pulses by solving equations involving only q and x, effectively decoupling the optimization process from the specific dynamic phase behavior imposed by the pulse shape.

Acknowledgements

Project supported by the Fundamental and Interdisciplinary Frontier Research Priority Program of the Chinese Academy of Sciences (Grant No. XDB0920000), the National Natural Science Foundation of China (Grant No. 12275331), and the Fund from the Penghuanwu Innovative Research Center (Grant No. 12447101).

References

[1] Peik E and Okhapkin M 2015 *Comptes Rendus. Physique* **16** 516
[2] Zhang C, Ooi T, Higgins J S, Doyle J F, von der Wense L, Beeks K, Leitner A, Kazakov G A, Li P, Thirolf P G, Schumm T and Ye J 2024 *Nature* **633** 63
[3] Xiao Q, Penyazkov G, Li X, Huang B, Bu W, Shi J, Shi H, Liao T, Yan G, Tian H, Li Y, Li J, Lu B, You L, Lin Y, Mo Y and Ding S 2026 *Nature* **650** 852
[4] Tiedau J, Okhapkin M V, Zhang K, Thielking J, Zitzer G, Peik E, Schaden F, Pronebner T, Morawetz I, De Col L T, Schneider F, Leitner A, Pressler M, Kazakov G A, Beeks K, Sikorsky T and Schumm T 2024 *Phys. Rev. Lett.* **132** 182501
[5] Elwell R, Schneider C, Jeet J, Terhune J E S, Morgan H W T, Alexandrova A N, Tan H B T, Derevianko A and Hudson E R 2024 *Phys. Rev. Lett.* **133** 013201
[6] Levitt M H 1986 *Progress in Nuclear Magnetic Resonance Spectroscopy* **18** 61
[7] Levitt M H 2008 *Spin Dynamics: Basics of Nuclear Magnetic Resonance*, 2nd edn. (Chichester, UK: John Wiley & Sons)
[8] Freeman R, Kempsell S P and Levitt M H 1980 *Journal of Magnetic Resonance* (1969) **38** 453
[9] Timoney N, Elman V, Glaser S, Weiss C, Johanning M, Neuhauser W and Wunderlich Chr 2008 *Phys. Rev. A* **77** 052334
[10] Mount E, Kabytayev C, Crain S, Harper R, Baek S Y, Vrijsen G, Flammia S T, Brown K R, Maunz P and Kim J 2015 *Phys. Rev. A* **92** 060301
[11] Butts D L, Kotru K, Kinast J M, Radojevic A M, Timmons B P and Stoner R E 2013 *J. Opt. Soc. Am. B* **30** 922
[12] Dunning A, Gregory R, Bateman J, Cooper N, Himsworth M, Jones J A and Freegarde T 2014 *Phys. Rev. A* **90** 033608
[13] Gustavsson S, Zwier O, Bylander J, Yan F, Yoshihara F, Nakamura Y, Orlando T P and Oliver W D 2013 *Phys. Rev. Lett.* **110** 040502
[14] Wang X, Bishop L S, Kestner J P, Barnes E, Sun K and Das Sarma S 2012 *Nat. Commun.* **3** 997
[15] Rong X, Geng J, Shi F, Liu Y, Xu K, Ma W, Kong F, Jiang Z, Wu Y and Du J 2015 *Nat. Commun.* **6** 8748
[16] Hollenstein U, Schmutz H, Agner J A, Sommavilla M and Merkt F 2017 *J. Chem. Phys.* **146** 014201
[17] Chini M, Wang X, Cheng Y, Wang H, Wu Y, Cunningham E, Li P C, Heslar J, Telnov D A, Chu S I and Chang Z 2014 *Nat. Photon.* **8** 437
[18] Genov G T, Schraft D, Halfmann T and Vitanov N V 2014 *Phys. Rev. Lett.* **113** 043001
[19] Torosov B T and Vitanov N V 2019 *Phys. Rev. A* **100** 023410
[20] von der Wense L, Bilous P V, Seiferle B, Stellmer S, Weitenberg J, Thirolf P G, Pálffy A and Kazakov G 2020 *Eur. Phys. J. A* **56** 176
[21] Torosov B T and Vitanov N V 2011 *Phys. Rev. A* **83** 053420
[22] Bilous P, Bekker H, Berengut J, Seiferle B, von der Wense L, Thirolf P G, Pfeifer T, Crespo Lopez-Urrutia J R and Palffy A 2020 *Phys. Rev. Lett.* **124** 192502
[23] Porsev S G, Cheung C and Safronova M S 2021 *Quantum Sci. Technol.* **6** 034014
[24] Zhao C C, Li L, Li S M, Gong Q R, Zhang P X, Hang Y, Ma L S and Zhu S N 2026 *Chin. Phys. B* **35** 020602
[25] Xu Y L, Zheng H Y, Yu X C, Zhang Y H, Shi T Y and Tang L Y 2026 *Chin. Phys. B* **35** 023101
[26] Rosen N and Zener C 1932 *Phys. Rev.* **40** 502
[27] Rakreungdet W, Lee J H, Lee K F, Mischuck B E, Montano E and Jessen P S 2009 *Phys. Rev. A* **79** 022316